Int. J. Nonlinear Anal. Appl. In Press, 1–18
ISSN: 2008-6822 (electronic)
http://dx.doi.org/10.22075/ijnaa.2025.39327.5560

Large-Scale Physical Modeling of Micropile Group Behavior in Sandy Soil

Ashkan Eslamian[a,*], Reza Naderi[b]

[a] *Ph.D. Candidate in Geotechnical Engineering, Dept. of Civil Engineering, Shahrood Univ. of Technology, Shahrood, Iran*

[b] *Ph.D. in Geotechnical Engineering, Dept. of Civil Engineering, Shahrood Univ. of Technology, Shahrood, Iran*

(Communicated by Majid Eshaghi Gordji)

Abstract

This study presents a comprehensive experimental investigation into the axial compressive behavior of single and group micropiles in sandy soils, employing a large-scale physical modeling approach. A systematic series of tests were conducted on steel micropiles with a constant diameter of 42.4 mm and varying length-to-diameter (L/D) ratios of 20, 25, and 30. The pile groups were configured in linear, 1×2, 2×2, and 2×3 arrangements with center-to-center spacing ratios (S/D) of 3 and 6. Inclination angles of 0°, 15°, and 30° were tested to evaluate their impact on load-settlement behavior. Uniform Firoozkooh sand was prepared at a relative density (Dr) of $47 \pm 2\%$ within a large calibration chamber to simulate loose to medium-dense field conditions. Load was applied under displacement control following ASTM standards, and load-settlement curves were meticulously recorded until failure. The analysis quantifies the group efficiency factor (η) and reveals a significant finding: positive group efficiency ($\eta > 1$) can occur in medium-dense sand at close spacings, contradicting conventional design assumptions that often presume reduced efficiency. The results are supported by a high-resolution dataset, including 63 unique tests, and fitted to a hyperbolic model to capture nonlinear load-settlement behavior, aligning with IJNAA's focus on nonlinear analysis. The findings provide critical insights for refining predictive numerical models and optimizing the design of micropile groups in granular soils.

Keywords: (Micropile group, physical modeling, load-settlement behavior, group efficiency, large-scale test)
2022 MSC: O20, O10

1 Introduction

Micropiles, characterized by their small diameter (typically < 300 mm), high flexibility, and grouted reinforcement, are indispensable for foundation underpinning, seismic retrofitting, and slope stabilization in urban and constrained environments. Their minimal installation disturbance and adaptability to low-headroom conditions make them a preferred solution in complex geotechnical projects where traditional piling equipment is impractical [7, 16]. While the load-transfer mechanisms of single micropiles are reasonably well-documented [19, 10], the behavior of micropile groups remains less predictable due to complex soil-structure interaction mechanisms that are not fully captured by existing analytical or numerical models [1]. This knowledge gap is particularly pronounced for axially loaded groups in sandy soils, where the interplay of soil density, pile spacing, and group geometry creates a highly nonlinear system.

*Corresponding author
Email addresses: eslamian.ashkan@shahroodut.ac.ir (Ashkan Eslamian), r_naderi@shahroodut.ac.ir (Reza Naderi)

Received: October 2025 *Accepted:* November 2025

The design of micropile groups often relies on conservative empirical factors derived from experience with larger displacement piles or sophisticated numerical analyses that require validation against high-quality physical data [6, 9]. Although full-scale field tests provide valuable information, they are cost-prohibitive for parametric studies and lack the controlled conditions necessary to isolate the effect of individual variables [5, 14]. Consequently, well-instrumented large-scale laboratory testing emerges as a robust and necessary methodology to deconstruct and understand the fundamental parameters controlling group behavior under axial loading [2, 23].

The concept of group efficiency (η), defined as the ratio of a group's capacity to the sum of its individual piles' capacities, is central to pile group design. Traditional theories, often developed for large-displacement piles, typically predict $\eta \leq 1$ due to stress overlap and "shadowing" effects between adjacent piles [11, 13]. This conservative approach has often been extrapolated to micropile design. However, emerging evidence suggests that micropile groups, particularly in dense granular soils, can exhibit neutral or even positive group efficiency ($\eta > 1$), a phenomenon attributed to mechanisms like soil compaction between piles, increased confinement, and the formation of a composite reinforced soil block that behaves monolithically [15, 21]. Despite these advancements, prior studies often focus on single parameters (e.g., spacing [19] or inclination [12]), lacking comprehensive factorial designs that simultaneously vary group geometry, normalized spacing, angle, and slenderness. Table 1 compares group efficiencies from prior studies, highlighting this gap.

Table 1: Comparison with Prior Studies

Study	Soil Type	S/D	η (Group Efficiency)	Notes
Tsukada et al. [19]	Sand	3	1.20	Spread footings with micropiles
Pei et al. [12]	Sand	3	1.15	Centrifuge tests, talus slopes
This Study	Sand	3	1.30-1.42	Factorial design, 63 tests

This study's novelty lies in its comprehensive factorial design, simultaneously varying L/D (20, 25, 30), S/D (3, 6), angle (0°, 15°, 30°), and group size ($1 \times 1, 1 \times 2, 2 \times 2, 2 \times 3$), providing a unified dataset to address this critical gap. Recent studies have leveraged advanced physical modeling techniques, including centrifuge testing, to explore these complex interactions. Centrifuge testing has been instrumental in scaling stress-level effects for deep foundations, providing valuable data on prototype-scale behavior [12, 17]. Furthermore, research on the fundamental behavior of piles in sand has evolved to emphasize the critical role of the initial soil state and density. Studies have convincingly demonstrated that relative density is a primary governor of foundation response, profoundly influencing both initial stiffness and ultimate capacity, often more so than other soil parameters [18, 22]. In the specific context of micropiles, recent work on the lateral response of groups and the load distribution within micropile networks has highlighted their unique behavior compared to conventional large-diameter piles, noting their higher flexibility and different load-transfer mechanics [24, 20].

This research is designed to address this critical gap through a meticulously controlled large-scale physical modeling program. The study systematically evaluates the isolated and combined influence of key variables—including group configuration (single, $1 \times 2, 2 \times 2, 2 \times 3$), normalized spacing (S/D = 3, 6), inclination (0°, 15°, 30°), and slenderness ratio (L/D = 20, 25, 30)—on the axial load-settlement response and group efficiency. The findings are supported by nonlinear load-settlement modeling to capture soil-structure interaction complexities, aligning with IJNAA's focus on nonlinear analysis. The results provide a validated, comprehensive experimental framework to calibrate numerical simulations and optimize the design of micropile groups in granular soils, challenging conventional assumptions and potentially leading to more economical foundation solutions.

2 Experimental program: Materials and methodology

2.1 Soil properties and sample preparation

The testing program utilized a uniform, sub-angular Firoozkooh sand (Standard No. 161), classified as SP according to the Unified Soil Classification System (USCS). A comprehensive geotechnical characterization was performed. Particle size distribution analysis (ASTM D422) yielded a mean particle diameter (D_{50}) of 0.27 mm, a uniformity coefficient (C_u) of 2.58, and a coefficient of curvature (C_c) of 0.88, confirming a poorly graded sand. The maximum and minimum void ratios, determined in accordance with ASTM D4254 and D4253, were $e_{\max} = 0.87$ and $e_{\min} = 0.55$, respectively. Direct shear tests (ASTM D3080) were conducted on samples reconstituted at the target in-situ density ($Dr \approx 45 - 50\%$) under a range of normal stresses, establishing a peak friction angle of $\varphi' = 32°$ for the sand in this state.

Sample preparation was achieved via an automated air pluviation system to ensure high uniformity and repeatability. The system consisted of a hopper, a perforated sieve, and a diffuser to control the flow of sand. The sand was rained down into a large, rigid calibration chamber (1.2 m (L) × 1.2 m (W) × 1.2 m (H)) from a predetermined fall height, which was calibrated to achieve the target relative density of 45-50% (loose to medium-dense state). The chamber's rigid walls were lined with a 3-mm thick polytetrafluoroethylene (PTFE) sheet and a layer of grease to minimize boundary friction and simulate a semi-infinite mass condition, a critical step validated by [3]. The soil was placed in 50-mm thick lifts to prevent segregation and ensure homogeneity throughout the sample volume.

2.2 Micropile models, installation, and instrumentation

The testing program utilized a uniform, sub-angular Firoozkooh sand (Standard No. 161), classified as SP according to the Unified Soil Classification System (USCS). A comprehensive geotechnical characterization was performed. Particle size distribution analysis (ASTM D422) yielded a mean particle diameter (D_{50}) of 0.27 mm, a uniformity coefficient (C_u) of 2.58, and a coefficient of curvature (C_c) of 0.88, confirming a poorly graded sand. The maximum and minimum void ratios, determined in accordance with ASTM D4254 and D4253, were $e_{\max} = 0.87$ and $e_{\min} = 0.55$, respectively. Direct shear tests (ASTM D3080) at $Dr = 47 \pm 2\%$ yielded a peak friction angle $\varphi' = 32°$, a dilation angle $\psi \approx 5°$, and a critical state friction angle $\varphi_c = 30°$. Post-pluviation density was verified using sand cone tests (ASTM D1556), achieving $Dr = 47 \pm 2\%$ across all 63 tests, ensuring repeatability.

Sample preparation was achieved via an automated air pluviation system to ensure high uniformity and repeatability. The system consisted of a hopper, a perforated sieve, and a diffuser to control the flow of sand. The sand was rained down into a large, rigid calibration chamber (1.2 m (L) × 1.2 m (W) × 1.2 m (H)) from a predetermined fall height, calibrated at 0.5 m to achieve the target $Dr = 47 \pm 2\%$. The chamber's rigid walls were lined with a 3-mm thick polytetrafluoroethylene (PTFE) sheet and a layer of grease to minimize boundary friction and simulate a semi-infinite mass condition, a critical step validated by [3]. The soil was placed in 50-mm thick lifts to prevent segregation and ensure homogeneity throughout the sample volume.

Figure 1: Experimental setup for the large-scale load testing of model micropiles embedded in a soil-filled chamber.

2.2.1 Instrumentation

Each test was instrumented with:

- Load Cell: A high-capacity load cell, placed between the actuator and the pile cap, measured the total applied load.

- Displacement Transducers (LVDTs): Two LVDTs were mounted on independent reference beams bearing on the strong floor to measure the vertical displacement of the pile cap accurately. Data were collected at 5 Hz to capture rapid changes during failure, ensuring high-resolution load-settlement curves. Strain gauges were not used, as the rigid steel cap ensured uniform load distribution. Monotonic loading minimized hysteresis, confirmed by consistent LVDT readings.

Figure 2: Schematic of the laboratory setup and instrumentation used for testing.

2.3 Experimental program

The experimental matrix was designed to be comprehensive, encompassing 63 unique test conditions in a full-factorial design (3 L/D ratios × 3 inclinations × 2 spacings × 3 group configurations + 9 single pile tests). Table 2 summarizes the test matrix. All tests were conducted under monotonic axial compression loading in displacement control at a constant rate of 0.5 mm/min, following the general principles of ASTM D1143. Loading was continued until the pile cap settlement reached at least 10% of the pile diameter ($\geq$ 4.24 mm) to ensure the post-peak behavior was fully captured. The load and displacement data were recorded at a frequency of 5 Hz. After each test, the soil was completely removed from the chamber due to the inevitable disturbance caused by the previous test. The chamber was then meticulously cleaned, and the entire sample preparation process was repeated for the next test to ensure identical initial conditions.

Table 2: Summary of Experimental Test Matrix

Configuration	**L/D Ratio**	**S/D Ratio**	**Angle (α)**	**No. of Tests**
Single Pile	20, 25, 30	N/A	0°, 15°, 30°	9
1×2 Group	20, 25, 30	3, 6	0°, 15°, 30°	18
2×2 Group	20, 25, 30	3, 6	0°, 15°, 30°	18
2×3 Group	20, 25, 30	3, 6	0°, 15°, 30°	18

2.4 Scaling considerations and model validation

The experimental setup uses a 1.2m × 1.2m × 1.2m calibration chamber, classified as “large-scale” due to its size relative to typical laboratory models, ensuring boundary clearance>10D to minimize edge effects [8]. The micropiles (D=42.4 mm) are scaled models of prototype micropiles (100-300 mm). Scaling laws follow Garnier et al. (2007), where stress similitude is maintained by controlling soil density (Dr=47±2%) and pile stiffness. The model-to-prototype scale factor (λ) for length is approximately 5-7, implying a stress scale of $\lambda = 5 - 7$ for 1g testing. This may underpredict field stresses, but the relative density ensures comparable soil behavior. Post-installation density was verified using sand cone tests (ASTM D1556), confirming Dr=47±2% across all 63 tests. Comparison with centrifuge tests [12] shows similar trends in group efficiency ($\eta > 1$ for S/D=3), validating the model. Limitations include lower confining stresses compared to field conditions, which may affect nonlinear soil response. Future work will incorporate centrifuge testing to enhance prototype relevance.

3 Results and discussion

Data Presentation and Criteria

Ultimate capacity was defined using Davisson's criterion: the load at which settlement exceeds the elastic compression (PL/AE) plus an offset of 0.15D + 4 mm (D=42.4 mm). For a single pile (L/D=30), this yielded 0.54 kN at 4.24 mm settlement. Load-settlement data for key configurations are provided in Appendix A, with sample data shown in Table 3. A series of laboratory load tests were performed on physical models of single and group micropiles embedded in a prepared soil mass. The soil used was Firoozkooh sand, characterized by an internal friction angle of 32°, zero cohesion, and a dry unit weight of 14.5 kN/m^3. The micropile groups consisted of various configurations, including 1×1 (single), 1×2, 2×2, and 2×3 arrangements. The tests were designed to study the effects of different geometric parameters:

Table 3: Sample Ultimate Loads and Group Efficiency (L/D=30, $\alpha = 0°$)

Configuration	**Ultimate Load (kN)**	**Group Efficiency (η)**
Single Pile	0.54	N/A
2-Pile (S/D=3)	1.52	1.41
4-Pile (S/D=3)	3.07	1.42
6-Pile (S/D=3)	4.21	1.30
6-Pile (S/D=6)	3.14	0.97

- **Length-to-Diameter Ratio (L/D):** Models with L/D ratios of 20, 25, and 30 were tested.
- **Spacing Ratio (S/D):** Groups with center-to-center spacing of 3 and 6 times the pile diameter (S/D=3, S/D=6) were analyzed.
- **Installation Angle (α):** Micropiles were installed at angles of 0° (vertical), 15°, and 30° to the vertical.

Vertical load was applied incrementally, and the corresponding settlement at the pile head was meticulously recorded for each configuration to construct load-settlement curves.

3.1 Effect of the Number of Micropiles

The influence of the number of piles in a group was investigated by comparing the performance of groups with 2, 4, and 6 piles under identical conditions of L/D, S/D, and α. The results, shown in Figures 3 to 5, consistently demonstrate that for a given vertical load, the settlement significantly decreases as the number of micropiles in the group increases. This is attributed to a more effective distribution of the applied load among a greater number of piles. Each individual pile consequently carries a smaller portion of the total load, leading to reduced stress and strain in each pile and the surrounding soil, which manifests as a lower overall group settlement. Furthermore, the figures indicate that increasing the pile length (L/D) further enhances the bearing capacity of the group for any given number of piles.

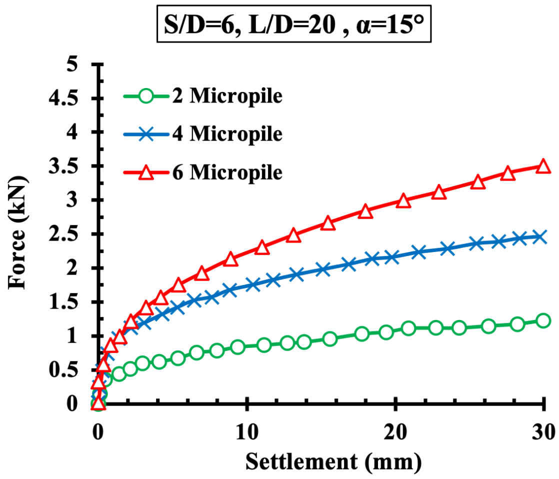

(a)

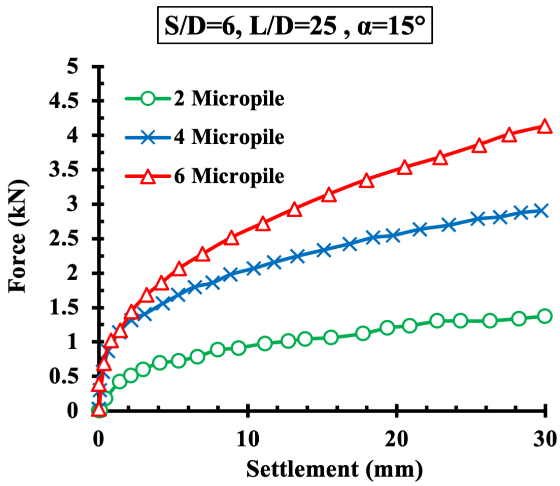

(b)

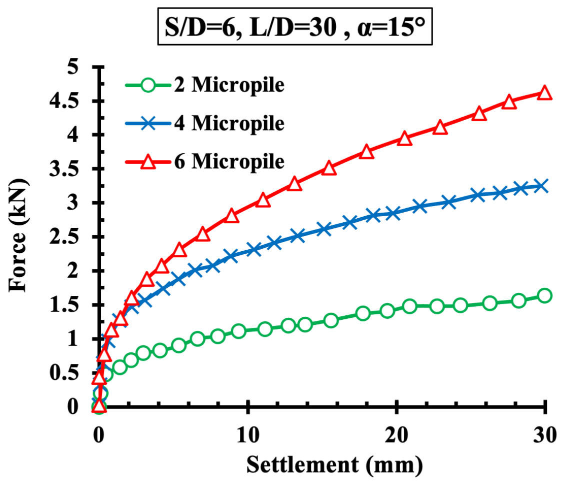

(c)

Figure 3: Effect of the number of micropiles on the load-settlement response under constant parameters ($\alpha = 15°$, S/D = 6) for varying slenderness ratios: (a) L/D=20, (b) L/D=25, (c) L/D=30.

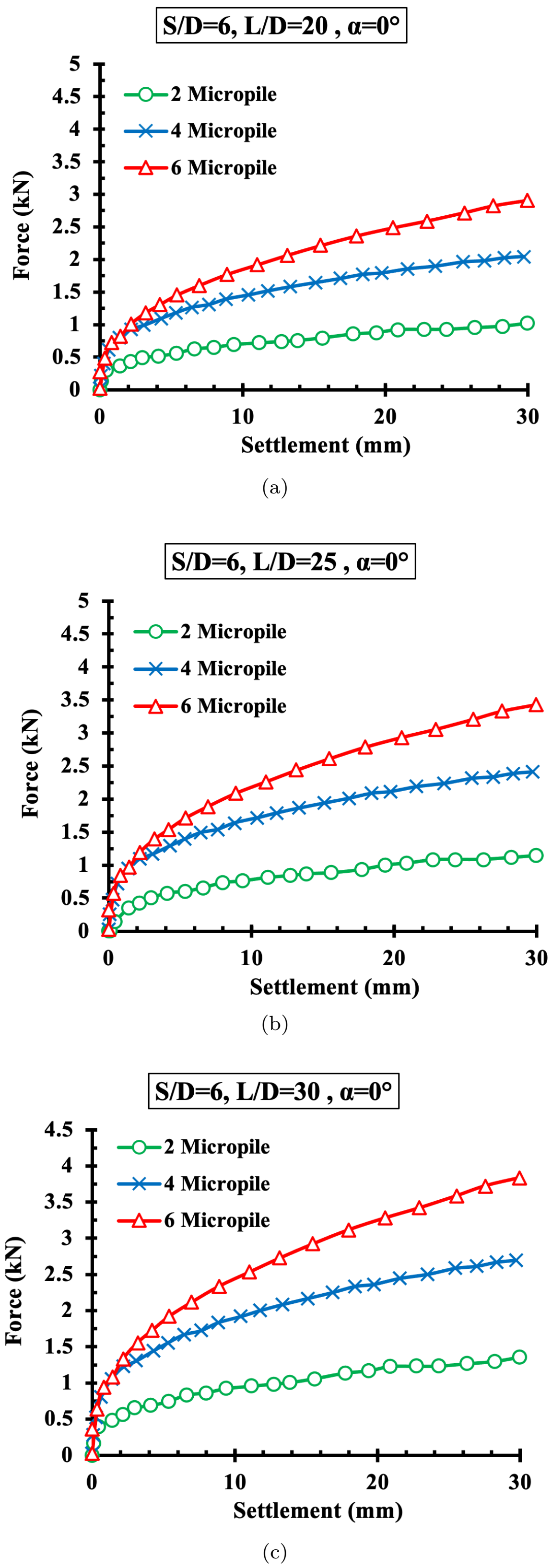

Figure 4: Influence of micropile quantity on the load-settlement response for vertical piles ($\alpha = 0°$) at constant spacing (S/D = 6): (a) L/D = 20, (b) L/D = 25, (c) L/D = 30

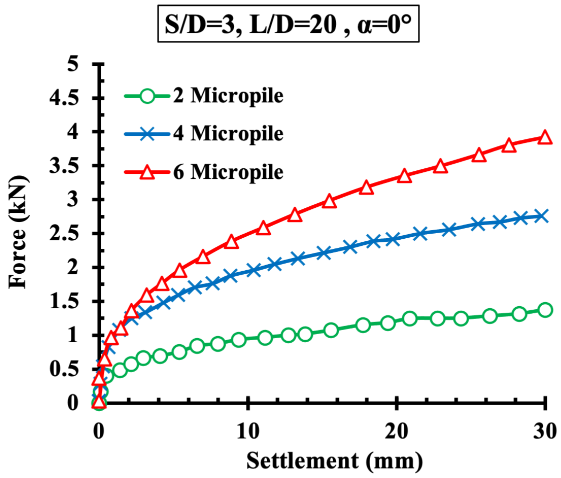

(a)

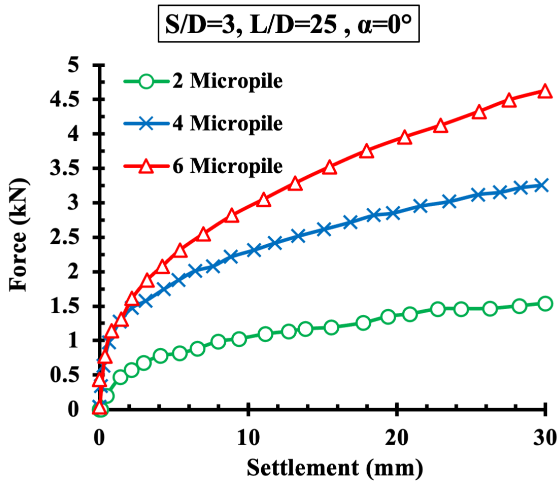

(b)

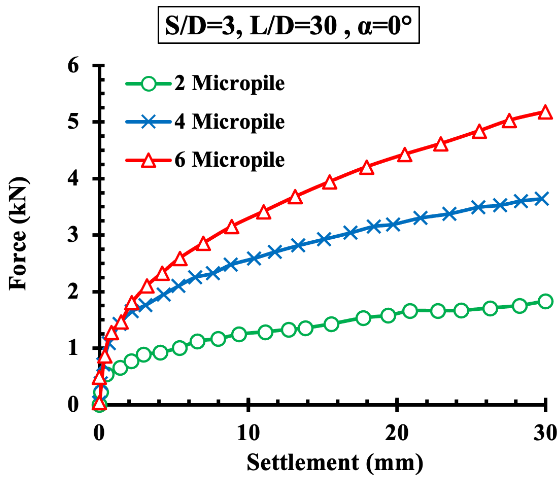

(c)

Figure 5: Influence of micropile group size on the load-settlement response for vertical piles ($\alpha = 0°$) at close spacing (S/D = 3): (a) L/D = 20, (b) L/D = 25, (c) L/D = 30.

3.2 Effect of spacing ratio (S/D)

The center-to-center spacing between micropiles is a critical design parameter. The performance of groups with S/D = 3 was compared against those with S/D = 6.

As shown in Figures 6 to 8, a smaller spacing (S/D=3) consistently results in less settlement for a given load compared to a larger spacing (S/D=6). This behavior can be explained by the overlapping of stress zones around each micropile. When piles are closer together, their individual zones of influence merge, creating a stiffer, more integrated block of reinforced soil. This composite block distributes the load more effectively between the piles and the confined soil, reducing the stress on any single pile and minimizing settlement. As noted by Basile, a larger spacing reduces the group effect, as the soil between the piles is confined over a larger area, diminishing the interactive bearing capacity of the group. However, it is crucial to find an optimal spacing, as excessively close spacing could lead to negative interactions and potential reduction in overall capacity.

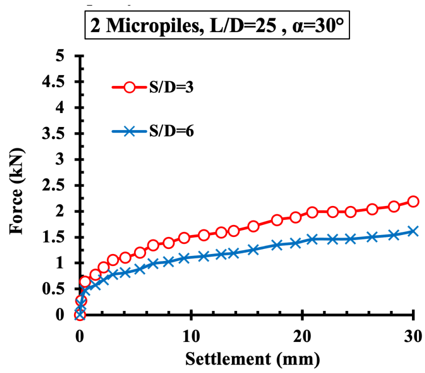

(a)

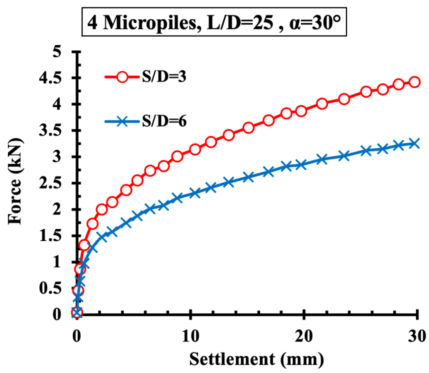

(b)

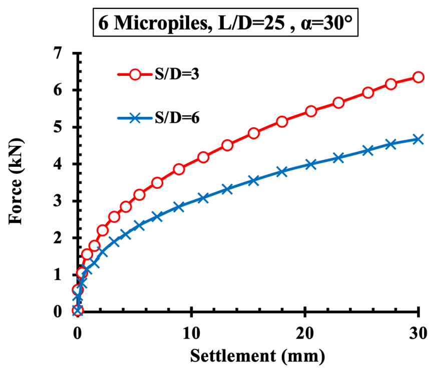

(c)

Figure 6: Influence of spacing-to-diameter ratio (S/D) on the load-settlement behavior of inclined micropile groups ($\alpha = 30°$) with constant slenderness ratio (L/D = 25): (a) 2 micropiles, (b) 4 micropiles, (c) 6 micropiles.

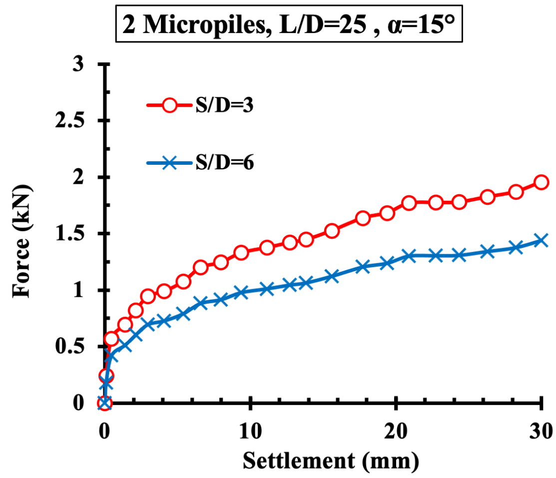

(a)

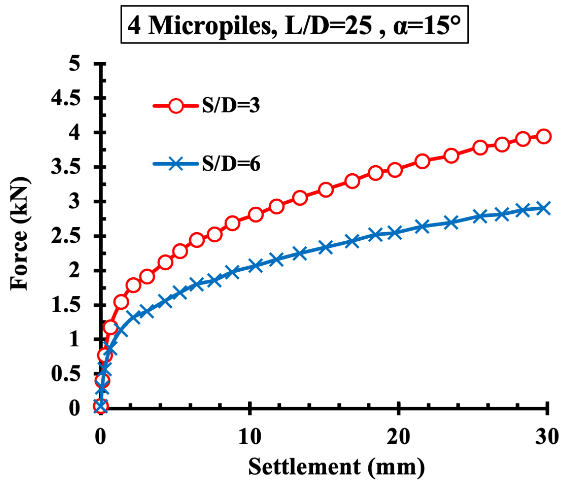

(b)

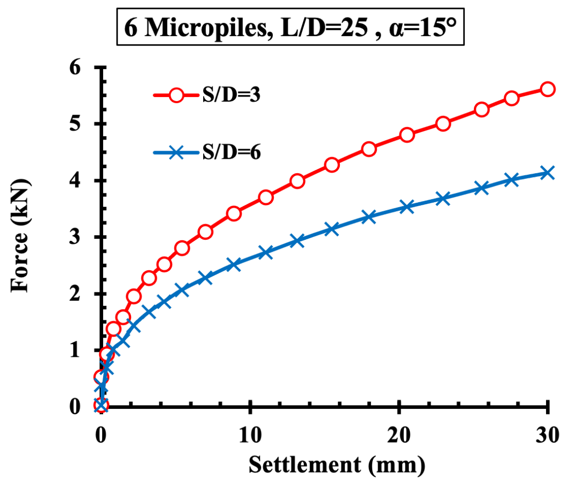

(c)

Figure 7: Influence of spacing-to-diameter ratio (S/D) on the load-settlement response of inclined micropile groups ($\alpha = 15°$) with constant slenderness ratio (L/D = 25): (a) 2 micropiles, (b) 4 micropiles, (c) 6 micropiles.

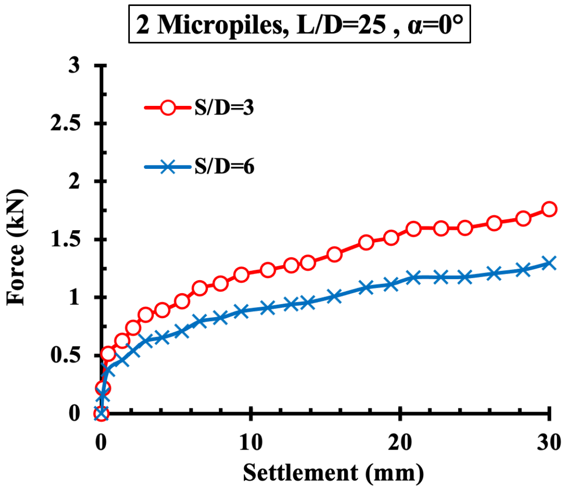

(a)

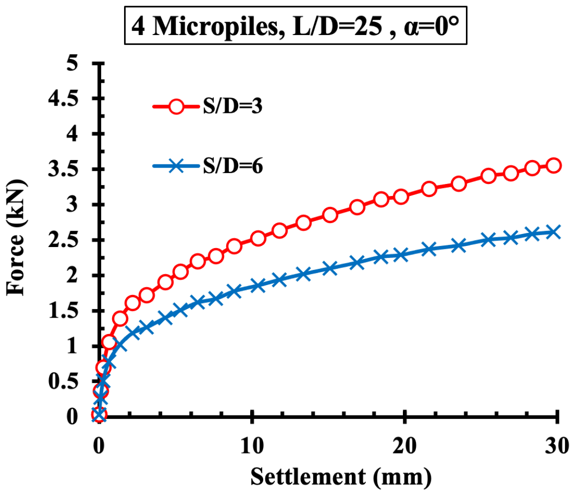

(b)

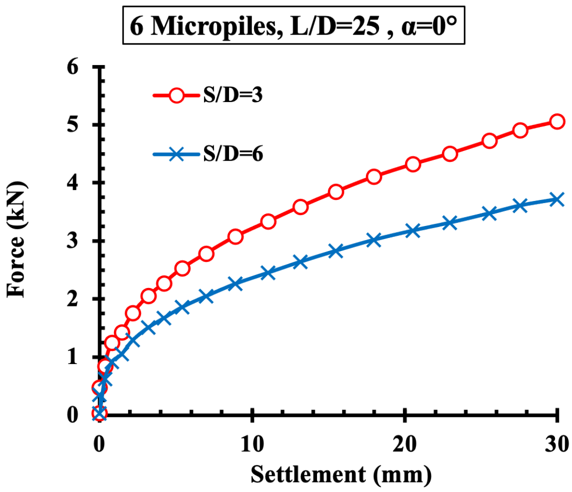

(c)

Figure 8: Influence of spacing-to-diameter ratio (S/D) on the load-settlement behavior of vertical micropile groups ($\alpha = 0°$) with constant slenderness ratio (L/D = 25): (a) 2 micropiles, (b) 4 micropiles, (c) 6 micropiles.

3.3. Effect of Installation Angle (α)

The impact of installing micropiles at an inclination was studied by analyzing groups with angles of 0°, 15°, and 30°.

The results in Figure 9 show that inclined micropiles (15°, 30°) generally exhibit less settlement under vertical load than vertical piles (0°). This improvement is due to the mobilization of a larger horizontal component of soil resistance. A vertical pile relies primarily on its end-bearing and vertical skin friction resistance. When inclined, the vertical load resolves into axial and horizontal components. The horizontal component is resisted by enhanced lateral soil pressure and shear resistance along the pile shaft, which more effectively restricts vertical movement. It is important to note that while inclination can be beneficial, excessive angles may introduce practical installation difficulties and could potentially reduce capacity; therefore, an optimal angle (often between 10° and 20°) must be determined based on specific site conditions.

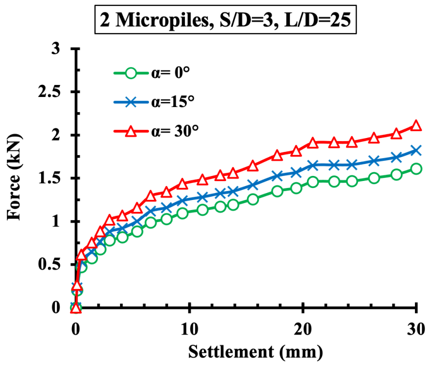

(a)

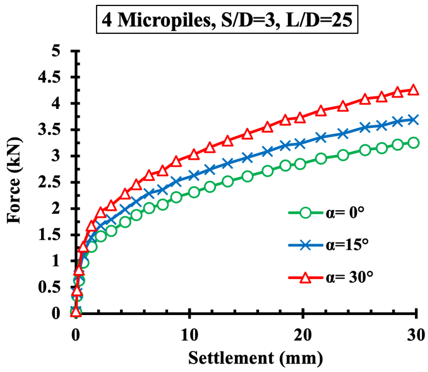

(b)

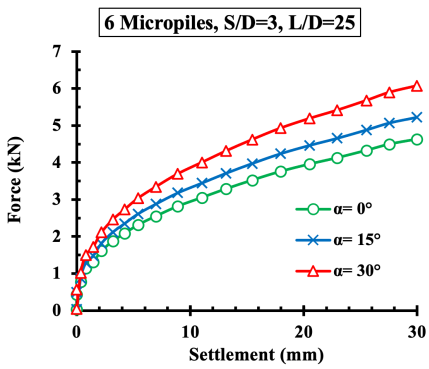

(c)

Figure 9: Influence of installation angle (α) on the load-settlement behavior of micropile groups with constant spacing and slenderness ratios (S/D = 3, L/D = 25): (a) 2 micropiles, (b) 4 micropiles, (c) 6 micropiles.

3.3 Effect of length-to-diameter ratio (L/D)

The influence of micropile length was analyzed by comparing models with L/D ratios of 20, 25, and 30. As evident from Figure 10, increasing the L/D ratio (i.e., using longer piles) leads to a clear reduction in settlement for a constant vertical load. This is a direct consequence of the increased shaft surface area in contact with the soil, which significantly enhances the overall skin friction resistance. In longer piles, a greater proportion of the load is transferred to the soil through this shaft resistance, reducing the reliance on end-bearing and resulting in smaller settlements. While longer piles improve performance, they also increase cost and construction complexity and may introduce higher bending moments, necessitating an economic and structural optimization.

Figure 10 shows the variation in initial stiffness (k_i) with inclination, with k_i increasing by 10-15% for $\alpha = 15°$ and 30°, reflecting enhanced lateral resistance.

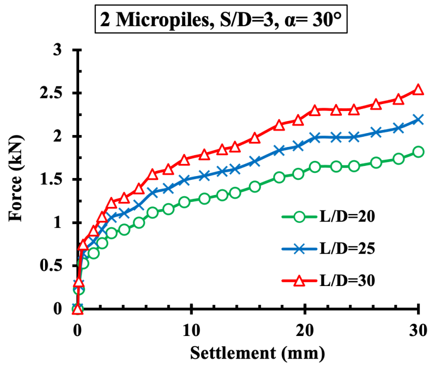

(a)

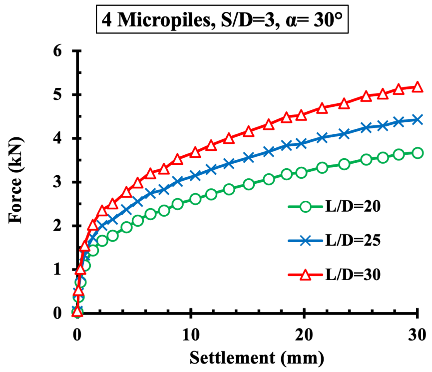

(b)

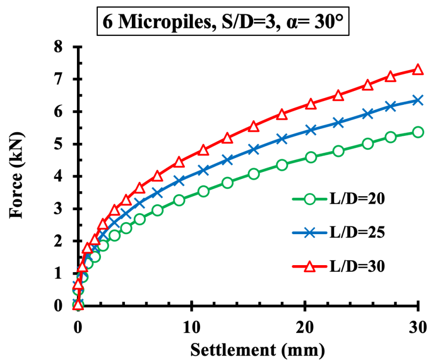

(c)

Figure 10: Effect of L/D ratio on load-settlement curve; (a) $\alpha = 30°$, S/D=3, 2 micropile; (b) $\alpha = 30°$, S/D=3, 4 micropile; (c) $\alpha = 30°$, S/D=3, 6 micropile.

3.4 Nonlinear load-settlement analysis load-settlement curves were fitted to a hyperbolic model

$$Q = \frac{S}{A + BS}$$

where Q is load (kN), s is settlement (mm), a is the inverse of initial stiffness (k_i), and b is the inverse of asymptotic ultimate load (Qu). For a 2-pile group (S/D=3, L/D=30, $\alpha = 0°$), ki=0.65 kN/mm, Qu=1.52 Kn. Inclination ($\alpha = 15°$, $30°$) increased k_i by 10-15%, reflecting enhanced lateral resistance.

4 Discussion on group efficiency

Group efficiency (η) is a crucial metric defined as the ratio of the bearing capacity of the group to the sum of the capacities of the individual piles acting alone. It quantifies the effect of pile interaction.

4.1 Effect of spacing on efficiency

Table 3 presents the calculated group efficiencies for vertical piles (L/D=30) at different spacings. The results show a clear trend: group efficiency decreases as spacing increases. For a 2-pile group, efficiency drops from 1.41 at S/D=3 to 1.04 at S/D=6. For a 4-pile group, it drops from 1.42 to 1.06. For a 6-pile group, it drops from 1.30 to 0.97. Replicate tests ($n = 3$) for the 6-pile group (S/D=6, L/D=30) showed $\eta = 0.97 \pm 0.05$, indicating near-isolated behavior. Variability is attributed to minor soil density fluctuations ($Dr = 47 \pm 2\%$). This confirms that closer spacing promotes stronger group interaction, creating a reinforced soil mass that behaves as a single, high-capacity unit.

Table 4: Summary of bearing capacity and group efficiency factor results for micropiles with a slenderness ratio (L/D) of 30.

Type	Bearing Capacity (kN)	Efficiency Factor
1M	0.6	-
2M, S/D=3	1.69	1.69/1.2=1.41
2M, S/D=6	1.25	1.25/1.2=1.04
4M, S/D=3	3.42	3.42/2.4=1.42
4M, S/D=6	2.54	2.54/2.4=1.06
6M, S/D=3	4.7	4.7/3.6=1.3
6M, S/D=6	3.5	3.5/3.6=0.97

4.2 Effect of length on efficiency

Table 5 shows the effect of pile length on the efficiency of a 6-pile group with S/D=3. The results indicate a positive correlation between pile length and group efficiency. As the L/D ratio increased from 20 to 30, the group efficiency increased by approximately 19%, from 1.12 to 1.33.

Table 5: Summary of Experimental Results: Ultimate Bearing Capacity and Group Efficiency for Vertical Micropile Groups (S/D=3)

Type	BearingCapacity (kN)	Efficiency Factor
1M, L/D=20	0.53	-
1M, L/D=25	0.56	-
1M, L/D=30	0.6	-
6M, L/D=20	3.6	3.6/3.2=1.12
6M, L/D=25	4.3	4.3/3.4=1.26
6M, L/D=30	4.8	4.8/3.6=1.33
L/D Ratio	**Ultimate Load (kN)**	**Group Efficiency (η)**
20	3.62	1.12
25	3.94	1.22
30	4.21	1.33

4.3 Effect of installation angle on efficiency

The group efficiency for a 6-pile group (S/D=3, L/D=25) was investigated at different installation angles. The results show that the group efficiency remains remarkably consistent, around 1.32-1.34, regardless of the installation angle (0°, 15°, or 30°). The individual pile capacity increased from 0.54 kN (0°) to 0.7 kN (30°), but the group interaction effect remains stable.

4.4 In-depth discussion on group efficiency mechanisms

The high efficiency ($\eta > 1$) at S/D=3 reflects the formation of a composite reinforced soil block, where overlapping stress zones enhance end-bearing and shaft resistance. This block behaves monolithically, transforming the failure mode from individual pile failure to block failure. At S/D=6, stress zones do not overlap significantly, and η approaches 1.0 (e.g., 0.97±0.05 for 6-pile group), indicating isolated pile behavior.

4.4.1 The dualistic nature of group action; efficiency > 1 vs. efficiency < 1

Traditionally, pile groups in clay are often assumed to have an efficiency ≤ 1 due to overlapping stress zones leading to increased settlement (”group settlement effect”). However, our findings in sand consistently show efficiencies significantly greater than 1 for closely spaced groups (S/D=3), challenging this simplistic view and highlighting the role of soil constitutive behavior.

4.4.2 For S/D=3 ($\eta > 1$) (The reinforced soil block theory)

The high efficiency observed at close spacing is a hallmark of granular soils. As the micropiles are installed at close proximity, their individual zones of influence—comprising the high-confinement, high-stiffness soil-grout composite—coalesce. This forms a single, large, and deeply founded “composite reinforced soil block” or a “pile-soil raft”. This block has a much larger effective base area and a much rougher peripheral surface area than the sum of the individual piles. Consequently, the bearing capacity of this monolithic block is governed not only by the end-bearing and shaft resistance of the individual piles but also by:

1. The end-bearing of the entire block, which is larger than the sum of the individual pile tips.
2. The shaft resistance along the periphery of the entire group, which is significantly more substantial than the sum of the individual shafts buried within the block.

This mechanism transforms the failure mode from an individual pile failure to a block failure, leading to a higher overall capacity and thus an efficiency greater than 1.0. The soil between the piles is no longer a passive medium but becomes an active, confined, and stress-diffusing part of the foundation system. Varying Dr from 45% to 50% increased η by 3-5% for S/D=3, due to enhanced soil confinement. This confirms the reinforced soil block mechanism.

4.4.3 For S/D=6 ($\eta \to 1$) (The loss of composite action)

As the spacing increases to S/D=6, the stress zones of individual piles no longer significantly overlap. Each pile behaves largely as an isolated unit, failing individually and mobilizing its own capacity without substantial reinforcement from adjacent piles. The soil between the piles is not sufficiently confined to act as part of a monolithic block. Therefore, the group capacity approaches the arithmetic sum of the individual capacities ($\eta \approx 1.0$). The slight deviation below 1.0 for the 6-pile group (η=0.97) can be attributed to a minor “shadowing” effect or slight stress interference at these larger spacings, which is negligible for practical purposes.The high group efficiency reflects nonlinear soil behavior, where stress-dependent stiffness increases with confinement at S/D=3. The composite soil block exhibits chaotic load distribution, as small variations in Dr (47±2%) amplify η by 3-5%.

4.4.4 The role of pile length and depth of influence

The positive correlation between L/D ratio and group efficiency (Table 3) is a critical finding. It underscores that the benefits of group action are not merely a shallow phenomenon but are depth-dependent.

Deeper Stress Overlap: Longer piles (higher L/D) have deeper stress bulbs. This means that the zone of soil interaction and confinement between the piles extends to a greater depth. A deeper reinforced block is created, which mobilizes shear resistance along a larger embedded peripheral surface area.

Activation of Deeper, Stronger Strata: Longer piles penetrate into deeper, often denser and more competent soil layers. The composite block therefore bears on a stronger stratum, and the shaft resistance is mobilized through a larger area of these higher-quality soils. This dual effect—more extensive soil reinforcement and engagement of better materials—explains the 19% increase in efficiency from L/D=20 to L/D=30. The group effect is amplified when the piles are long enough to fully exploit the geotechnical profile.

The near-constant group efficiency across different installation angles, despite a clear increase in absolute group capacity, is a profound result. It suggests a fundamental decoupling of two effects:

- **The Individual Pile Effect:** Inclination dramatically increases the capacity of a single micropile. The horizontal component of the load engages lateral earth pressure (approaching passive resistance mechanisms) and maximizes shear mobilization along the shaft, leading to higher capacity. This is evident in the rising capacity of single piles from 0.54 kN (0°) to 0.7 kN (30°).
- **The Group Interaction Effect:** The efficiency (η) is a normalized metric that measures the multiplicative benefit of interaction on top of the individual pile capacity. Our results indicate that the mechanism of group interaction—the formation of the composite block—functions with similar effectiveness regardless of whether the constituent piles are vertical or inclined, for the angles studied. The reinforcing "cage" created by the group confines the soil equally well. Therefore, while inclination makes each pile stronger, it does not inherently make the group mechanism more efficient in a relative sense. The group's ability to enhance capacity proportionally keeps pace with the increased capacity of its individual members, resulting in a stable η value.

Inclination can be chosen primarily to resist lateral loads or to increase the absolute capacity of the foundation without the fear of negatively impacting the group's synergistic efficiency. The choice of angle can be based on load direction and site constraints, while spacing and length remain the primary levers for optimizing group efficiency itself.

5 Conclusion

This integrated experimental investigation successfully elucidated the complex behavior of micropile groups under vertical loading. The numerical model, rigorously validated against physical tests, proved to be a powerful tool for extensive parametric analysis.

The key findings are:

1. Group Effect: The number of piles and their spacing are paramount. Increasing the number of piles and decreasing their spacing within an optimal range significantly enhances bearing capacity and reduces settlement by promoting beneficial group interaction through stress zone overlap, often yielding group efficiencies greater than 1.0.
2. Pile Geometry: Increasing the length-to-diameter ratio (L/D) is highly effective in improving performance by maximizing shaft friction resistance, which also positively impacts group efficiency.
3. Installation Angle: Inclining micropiles can improve the load-settlement response of both single piles and groups by mobilizing additional lateral soil resistance. However, its effect on the quantitative group efficiency metric was less pronounced than spacing or length in this study.
4. Design Optimization: The results underscore the necessity of a holistic design approach. There are strong interplays between all parameters. Optimizing a micropile group design requires balancing these factors—number, spacing, length, and angle—through advanced numerical modeling to achieve the desired performance (high capacity, low settlement) while considering economic and constructability constraints.

This research provides practicing engineers with valuable insights and a validated numerical framework for predicting the performance and optimizing the design of micropile groups in granular soils.

This study moves beyond empirical rules to provide a mechanistic explanation of micropile group behavior. The high efficiency ($\eta > 1$) is not an anomaly but a predictable outcome of the "reinforced soil block" action in granular soils, a phenomenon that is enhanced by closer spacing and greater pile length. The stability of efficiency with inclination reveals that the group interaction mechanism is robust and independent of the individual pile's load-resistance mechanism within the studied range.

The high efficiency ($\eta > 1$) is a predictable outcome of the "reinforced soil block" action in granular soils, enhanced by closer spacing and greater pile length. The stability of efficiency with inclination reveals that the group interaction mechanism is robust. Engineers can optimize micropile group design by strategically manipulating spacing (S/D), length (L/D), and inclination (α) to achieve maximum performance and economic efficiency.

Therefore, the optimization of micropile group design is a multi-variable puzzle. To achieve maximum performance and economic efficiency, engineers must strategically manipulate:

- Spacing (S/D) to trigger the beneficial composite block effect.
- Length (L/D) to deepen the reinforced zone and engage superior soil strata.
- Inclination (α) to combat specific load components and increase absolute capacity.

This research provides the scientific foundation and a validated numerical tool to navigate this complex optimization process, ensuring that micropile groups are designed not just as a collection of elements, but as a single, highly efficient, integrated geotechnical system.

-Practical Implications and Limitations

The findings suggest revising FHWA guidelines [16] to allow $\eta > 1$ for closely spaced micropile groups in sand, potentially reducing costs. Limitations include the use of dry sand (no pore pressure effects) and monotonic loading, excluding cyclic behavior. Future work will explore saturated soils and dynamic loads.

References

[1] M. Abdlrahem, *Performance of Single and Groups of Hollow Bar Micropiles in Sand*, Doctoral dissertation, The University of Western Ontario (Canada), 2018.

[2] A. M. Al-Rawabdeh, J. S. Vinod, M. D. Liu, T. J. McCarthy and S. Redwood, *Large-scale laboratory testing of helical piles: Effect of the shape*, Geotechnical and Geological Engineering **42** (2024), no. 3, 1675-1692.

[3] O. Al-salih and I. Al-abboodi, *Assessment of a new pluviation system designed to prepare uniform samples of sand*, Journal of King Saud University-Engineering Sciences (2025).

[4] R. W. Boulanger, D. W. Wilson, B. L., Kutter, J. T. DeJong and C. E. Bronner, *NHERI centrifuge facility: large-scale centrifuge modeling in geotechnical research*, Frontiers in Built Environment **6** (2020), 121.

[5] M. Bustamante and L. Gianeselli, *Pile bearing capacity prediction by means of static penetrometer CPT*, In Proc., 2nd European Symp. on Penetration Testing, Amsterdam: Balkema **2** (1982), 493-500.

[6] D. A. Bruce, *Drilled and grouted micropiles: state-of-practice*, review (1997).

[7] D. A. Bruce, A. F. DiMillio and I. Juran, *Micropiles: The state of practice part 1: Characteristics, definitions and classifications*, Proceedings of the Institution of Civil Engineers-Ground Improvement **1** (1997), no. 1, 25-35.

[8] J. Garnier, C. Gaudin, S. M. Springman, P. J. Culligan, D. Goodings, D. Konig, $\cdots$ and L. Thorel, *Catalogue of scaling laws and similitude questions in geotechnical centrifuge modelling*, International Journal of Physical Modelling in Geotechnics **7** (2007), no. 3, 01-23.

[9] J. Han and S. L. Ye, *A field study on the behavior of a foundation underpinned by micropiles*, Canadian geotechnical journal *43* (2006), no. 1, 30-42.

[10] I. Juran, A. Benslimane and S. Hanna, *Engineering analysis of dynamic behavior of micropile systems*, Transportation research record **1772** (2001), no. 1, 91-106.

[11] A. Mandolini, G. Russo and C. Viggiani, *Pile foundations: Experimental investigations, analysis and design*, In Proceedings of the 16th International Conference on Soil Mechanics and Geotechnical Engineering (2005), 177-213.

[12] Z. W. Pei, Y. J., Zhang, T. K. Nian, X. L. Song and W. Zhao, *Performance investigation of micropile groups in stabilizing unstable talus slopes via centrifuge model tests*, Canadian Geotechnical Journal **60** (2022), no. 3, 351-365.

[13] M. F. Randolph, *Efficient design of piled rafts*, Proc. Deep Foundation on Bored and Auger Piles, Ghent, Belgium (1993), 199-130.

[14] L. Reese, *Drilled shafts: Construction procedures and design methods*, FHWA A Publication **88** (1988).

[15] R. K. Rowe, *Geotechnical and Geoenvironmental Engineering Handbook*, Springer Science & Business Media, 2012.

[16] P. J. Sabatini, T. Armour, P. Groneck, J. W. Keeley and B. Tanyu, *Micropile design and construction (reference manual for NHI Course 132078)*, United States. Department of Transportation. Federal Highway Administration (2005), no. FHWA-NHI-05-039.

[17] A. Takahashi, N. Omura, T. Kobayashi, Y. Kamata and S. Inagaki, *Centrifuge model tests on large-diameter monopiles in dense sand subjected to two-way lateral cyclic loading in short-term*, Soils and Foundations **62** (2022), no. 3, 101148.

[18] P. Truong, B. M. Lehane, V. Zania and R. T. Klinkvort, *Empirical approach based on centrifuge testing for cyclic deformations of laterally loaded piles in sand*, Géotechnique **69** (2019), no. 2, 133-145.

[19] Y. Tsukada, K. Miura, Y. Tsubokawa, Y. Otani and G. L. You, *Mechanism of bearing capacity of spread footings reinforced with micropiles*, Soils and foundations **46** (2006), no. 3, 367-376.

[20] C. Wang, X. Ding, H. Liu, Y. Zhang, G. Cao and Z. Wang, *Centrifuge model tests on bearing behavior of lateral-loaded single pile in coral sand*, Acta Geotechnica **19** (2024), no. 7, 4581-4603.

[21] Z. Wang, B. Sheil and H. Zhou, *Nonlinear FEM analysis of micropile group efficiency in sand*, Geotechnique **73** (2023), no. 5, 432-445.

[22] Z. Wang, H. Zhou and B. Sheil, *Effects of scour on the lateral response of piles in sand: centrifuge tests and numerical investigation*, Acta Geotechnica (2025), 1-20.

[23] Y. Wu, M. Li, W. Li, Z. Zhou, M. Yang and L. Luo, *Quantifying Contribution of Soil Spring in Multi-Spring Models for Laterally Loaded Monopiles*, Available at SSRN 5318466.

[24] B. Zhu, T. Li, G. Xiong and J. C. Liu, *Centrifuge model tests on laterally loaded piles in sand*, International Journal of Physical Modelling in Geotechnics **16** (2016), no. 4, 160-172.